

## Scaling law in liquid drop coalescence driven by surface tension

Mingming Wu<sup>a)</sup>

*Department of Physics, Occidental College, Los Angeles, California 90041  
and Mechanical and Aerospace Engineering Department, Cornell University, Ithaca, New York 14853*

Thomas Cubaud and Chih-Ming Ho

*Mechanical and Aerospace Engineering Department, University of California at Los Angeles, Los Angeles, California 90095*

(Received 24 February 2004; accepted 9 April 2004; published online 18 May 2004)

This Letter reports experimental results on the coalescence of two liquid drops driven by surface tension. Using a high speed imaging system, we studied the early-time evolution of the liquid bridge that is formed upon the initial contact of two liquid drops in air. Experimental results confirmed the scaling law that was proposed by Eggers *et al.* based on a simple and yet elegant physical argument. We found that the liquid bridge radius  $r_b$  follows the scaling law  $r_b \propto t^{1/2}$  in the inertial regime. Further experiments demonstrate that such scaling law is robust when using fluids of different viscosities and surface tensions. The prefactor of the scaling law,  $r_b/t^{1/2}$ , is shown to be  $\propto R^{1/4}$ , where  $R$  is the inverse of the drop curvature at the point of contact. The dimensionless prefactor is measured to be in the range of 1.03–1.29, which is lower than 1.62, a prefactor predicted by the numerical simulation of Duchemin *et al.* for inviscid drop coalescence. © 2004 American Institute of Physics. [DOI: 10.1063/1.1756928]

When two liquid drops approach each other with negligible initial velocities, van de Waals force joins the two drops together and forms a tiny liquid bridge. The bridge, due to its large curvature, quickly expands under the influence of interfacial stress and the resultant fluid motion pulls two drops together and forms a larger drop with smaller surface area. A movie of this process can be viewed at <http://www.oxy.edu/~mingming/coalescence.html>. Much of the early experimental and theoretical work on drop coalescence is motivated by its applications in industrial processes (printing and sintering processes), as well as its fundamental importance as a free surface problem in fluid dynamics.<sup>1–5</sup> Recently, liquid drop coalescence has been brought into new light due to its applications in microfluidic device for biochemical reactions.<sup>6–8</sup> In a digital microfluidic platform, small volumes of fluids are manipulated in the form of droplets on a flat substrate. These small droplets, diameter ranges from a few hundreds  $\mu\text{m}$  to a few mm, can be merged, transported and separated on a substrate via external forces (electrowetting force and thermocapillary force, for example). Such a device is an especially promising contender for automating chemical and biological experiments, or for a  $\mu\text{TAS}$  (micro total analysis system). Important questions to ask are how well the contents of two drops mix when they merge, and whether the surface tension driven flow during drop coalescence can be utilized to enhance mixing. It is in this context that we wish to understand the early dynamical processes of the liquid drop coalescence.

The problem of liquid drop coalescence driven by surface tension has been studied in detail both analytically and

numerically by Eggers *et al.*<sup>2</sup> Their work focuses on the viscous regime when the Reynolds number  $Re \ll 1$ , and the dynamical process can be described by a set of Stokes equations. The Reynolds number of the surface tension driven flow is defined as  $Re = \sigma r_b / (\rho \nu^2)$ , where  $r_b$  is the radius of the bridge along the initial contact line [see Fig. 1(b)],  $\sigma$  is the surface tension,  $\rho$  is the density, and  $\nu$  the kinetic viscosity of the liquid drop. The early time evolution of the shape of the liquid bridge is revealed, and the bridge radius  $r_b$  is shown to follow a scaling law of  $r_b \propto t \ln(t)$ .

While the study of the viscous regime is critical in understanding drop coalescence involving high viscosity fluids, such as the sintering process (forming a homogenous material by heating glass powder or metal powder), it is of less relevance to coalescence problems occurring in biology and chemistry experiments where low viscosity fluids are often involved. For instance, the bridge radius  $r_b$  needs to be less than 10 nm in order for the Reynolds number to be less than 1 using water drops. It is thus important to treat the problem in the inertial regime, when  $Re \gg 1$ . In the inertial regime, Eggers *et al.* further proposed a scaling law based on a simple physical argument.<sup>2</sup> Assuming that the interfacial stress is set by the smallest length scale—the gap width  $\Delta$  [see Fig. 1(b)], the interfacial stress that drives the bulk fluid motion is then  $\sigma/\Delta$ . Balancing the kinetic energy and the interfacial stress, one gets  $(1/2)\rho v^2 \propto \sigma/(r_b^2/2R)$ , where  $v$  is the characteristic velocity of the bulk fluid near the bridge. This leads to the scaling law of  $r_b \propto (R\sigma/\rho)^{1/4} t^{1/2}$ . Duchemin *et al.* further carried out a numerical simulation on the early time evolution of the liquid bridge for inviscid drop coalescence. In addition to confirming the above scaling law, they found the prefactor to the above scaling law to be 1.62. Rewriting the scaling law in dimensionless form, one gets

<sup>a)</sup> Author to whom correspondence should be addressed. Electronic mail: [mw272@cornell.edu](mailto:mw272@cornell.edu)

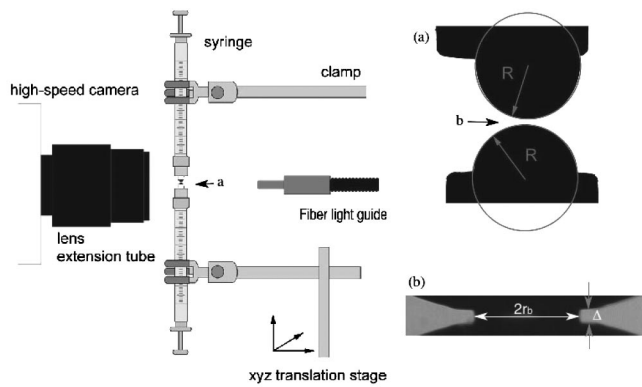


FIG. 1. Schematics of the drop coalescence experiment. (a) is an image of the two drops before merging, the inverse of the drop curvature is measured as shown ( $R=0.139$  cm); (b) shows the area close to the point of contact shortly after the drops are merged, the size of the image is  $0.204 \times 0.0245$  cm.  $2r_b$  is the width of the bridge along the initial contact line and  $\Delta$  is the bridge gap width.

$r_b/R = 1.62(t/\tau)^{1/2}$ , where  $\tau = \sqrt{(\rho R^3)/\sigma}$  is the characteristic time in inviscid flow. Note that the numerical simulation is carried out in the parameter regime of  $r_b/R < 0.035$ .

Very little experimental work has been done to study the liquid drop coalescence in the inertial regime due to its rapid motion.<sup>9</sup> The time scale for merging two 0.1-cm radius drops in inertial regime is set by  $\sqrt{(\rho R^3)/\sigma}$ , which is about 4 ms for water. One exception is the work of Menchaca-Rocha *et al.*,<sup>4</sup> where mercury drops are used together with a high speed video camera. The experimental data supported the  $r_b \propto t^{1/2}$  scaling law. However, the main focus of their work is on the time evolution of the overall drop shape during the coalescence. Several aspects of the problem surrounding the early time evolution of the drop coalescence, such as the influence of fluid properties and the dependency of the scaling law prefactor on drop size, have never been checked by experiments. This Letter presents an experimental study on the early time evolution of the bridge contours formed by merging two liquid drops in air using three commonly used fluids; water, water-glycerol mixture, and methanol. In addition to confirming the bridge width scaling law  $r_b \propto t^{1/2}$ , we further provide the detailed bridge contour images during the initial drop merging process, as well as quantitative measurements of the prefactor of the scaling law.

The experiment is set up in such a way that the two liquid drops are made to merge in air with negligible initial velocities (see Fig. 1). Small drops (from 0.05 to 0.15 cm) are produced using a 250  $\mu$ l SGE Gas-Tight syringe and larger drops (from 0.15 to 0.3 cm) are produced using a 10 ml Upchurch Scientific disposable syringe. Due to contact angle hysteresis, the contact line between the drop and the syringe tip is pinned between the receding and the advancing contact angle. The drop curvature can thus be adjusted by carefully changing its volume with the syringe piston. The largest pendant drop obtainable is about the capillary length  $\lambda_c = (\sigma/g\rho)^{1/2}$ , which is about 0.3 cm for water. The drops are backlit by a quartz halogen fiber optic illuminator (Dolan-Jenner MI-150, 150 W) through an optic fiber light guide. The diameter of the optical fiber bundle is 5 mm. A

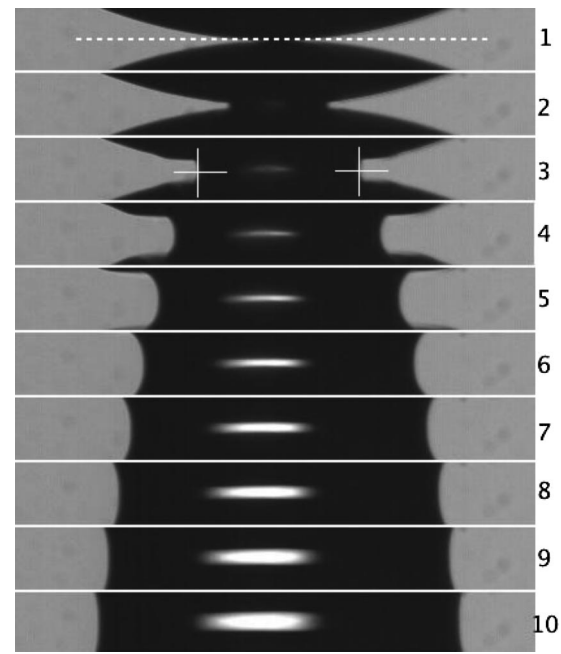


FIG. 2. Ten consecutive images (100  $\mu$ s apart) taken by the high speed camera. The size of each image is  $400 \times 48$  pixels which corresponds to  $0.204 \times 0.0245$  cm. Water drop of radius 0.191 cm is used. Dashed line is the initial contact line. The two crosses mark the locations of the bridge's front  $r'$ .

high speed camera (Redlake, MotionPro) is used to record the dynamics of drop coalescence. The full spatial resolution of the camera is  $1280 \times 1024$  pixels, and it varies with the acquisition speed. All the images (except for those noted) are taken at 10 k frames per second, with spatial resolution of  $384 \times 48$  pixels,  $512 \times 48$  pixels and 10  $\mu$ s exposure time. A 60 mm Nikon macrolens is mounted either directly or via an extension tube to the high-speed camera.

For each experimental run, we first manually make two drops of equal size at the tips of the syringes. Second, we fix the location of the pendant drop and adjust the macrolens until the outline of the pendant drop is in focus. Third, the position of the lower drop is adjusted using a  $xyz$  microtranslation stage ( $0.5 \mu$ m per line resolution) until it is very close to the pendant drop and it is in focus. Finally, the lower drop is moved up slowly until it touches the pendant drop. The axisymmetric nature of the system ensures that the outline of the liquid bridge is always in focus during the experimental run, as shown in Fig. 2. The curvatures of the drops are obtained using images that are taken by the camera with full resolution right before the drops are merged [see Fig. 1(a)]. Experiments were carried out at room temperature  $20 \pm 0.5$   $^\circ$ C.

Three different fluids are used to make drops. First, we used deionized water (UCLA, Nanoelectronics research facility). The surface tension of the water is 72.7 dyn/cm, density is 0.998 g/cm<sup>3</sup> and viscosity is 1.00 cP. Second, we used methanol (EM science). The surface tension of methanol is 22.7 dyn/cm, density is 0.792 g/cm<sup>3</sup> and viscosity is 0.59 cP. Third, we used deionized water and glycerol (Fisher Scientific) mixture (composition: 60% glycerol, 40% water in vol-

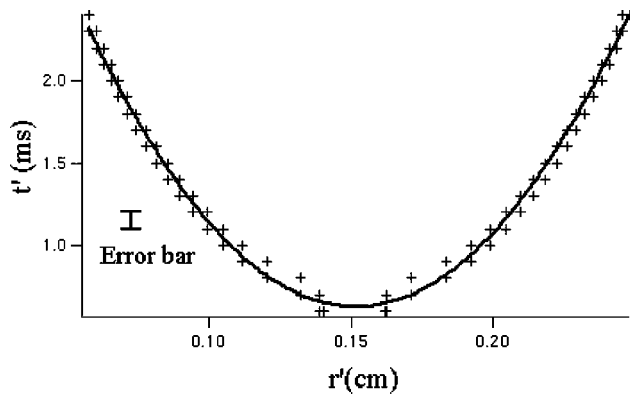


FIG. 3. The locations of bridge's front  $r'$  at various time  $t'$ . Data are extracted from image series shown in Fig. 2. + is experimental data and line is a fit to  $t' = t'_0 + A*(r' - r'_0)^2$ , where  $t'_0$ ,  $r'_0$  and  $A$  are fitted parameters.

ume), with a surface tension of 67.4 dyn/cm, a density of 1.16 g/cm<sup>3</sup> and a viscosity of 14.4 cP.<sup>10,11</sup>

For each experimental run, a movie series of  $\sim 50$  frames is taken and saved on the computer hard disk for later analysis. Figure 2 is a sequence of images taken within the first millisecond after two water drops merge. The bright spot in the middle of the image is caused by the lens effect of the cylindrical liquid bridge. The two drops make the initial contact sometime between frame 1 and frame 2, and a liquid bridge is clearly formed in frame 2. The liquid bridge expands rapidly in the first few frames, and slows down in the later frames, which is consistent with the  $t^{1/2}$  scaling law. An image processing software ImageJ (NIH) is used to find the bridge width at various time. We first plot the space time diagram of the image line along the initial drop contact line [dashed line in Fig. 2] from the image sequence. The locations of the bridge's front  $r'$  (see crosses in Fig. 2) at various time  $t'$  are then obtained by finding the edges of the resultant space time diagram, and the result is shown in Fig. 3. Due to the rapid dynamics in the initial stage of the coalescence, it is important to locate the initial drop contact time accurately. The following procedure is adopted for obtaining the initial time. We fit the experimental data in Fig. 3 to a function  $t' = t'_0 + A*(r' - r'_0)^2$ , and fitted parameters  $t'_0$  and  $r'_0$  are used as initial time and center of the bridge, respectively. The time  $t$  is then defined as  $t = t' - t'_0$ , and bridge radius  $r_b = |r' - r'_0|$ . Figure 4 shows plots of dimensionless bridge width  $r_b/R$  as a function of the square root of the dimensionless time  $(t/\tau)^{1/2}$  for water drops of various radii (0.05–0.35 cm). Data sets taken from different drop radii collapse well into one line when plotted in dimensionless form. This demonstrates that  $r_b/R \propto (t/\tau)^{1/2}$ , which leads to  $r_b/t^{1/2} \propto R/\tau^{1/2} \propto R^{1/4}$ , as predicted by the theory of Eggers *et al.*

The uncertainty of the time measurement is 100  $\mu$ s, which is determined by the frame rate of the camera. This is shown by the error bar in Fig. 3. The uncertainty in length measurement is one pixel, which is 2.10–5.50  $\mu$ m depending on the magnification of the lens assembly. It is about the size of the symbol in Fig. 3. The limitation in time measurements shows up for data taken from smaller drops (see circles in Fig. 4), since the characteristic time is  $\propto R^{3/2}$ . However, the

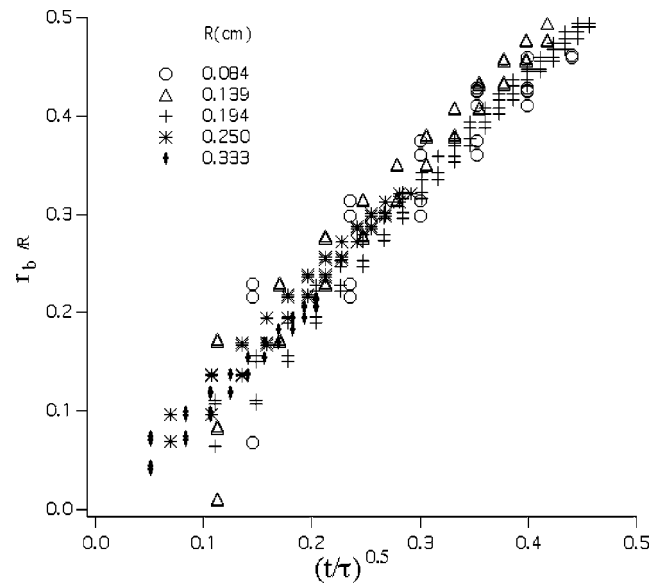


FIG. 4. Bridge width as a function of square root of time for water drops of various radii.

discreteness of the data did not affect its overall linear nature as shown in Fig. 4.

The above experiments were repeated using glycerol–water mixture (viscosity  $\sim 14.4$  times that of water), and methanol (surface tension  $\sim 1/3$  that of water). The results are shown in Fig. 5. In all cases, the bridge width scaling law  $r_b \propto t^{1/2}$  is followed, and the dimensionless prefactor is independent of drop radius supporting the relation  $r_b/t^{1/2} \propto R^{1/4}$ . The average dimensionless prefactor for methanol is  $1.29 \pm 0.05$ , water–glycerol mixture  $1.03 \pm 0.07$ , and water  $1.09 \pm 0.08$ . The dimensionless prefactors for water and water–glycerol drop coalescence are the same within the experimental errors. The dimensionless prefactor for methanol, however, is about 20% higher. The differences of drop coalescence using different fluids also show up in the shape of the interface between the air and the drop near the liquid bridge as shown in Fig. 6. Capillary waves are clearly seen travelling along the air drop interface for methanol and water drops, while absent in the case of water–glycerol mixture

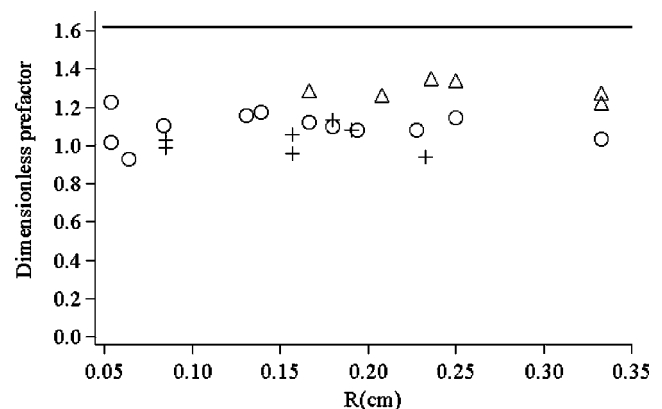


FIG. 5. Scaling prefactors obtained from experiments using  $\circ$  water; + water–glycerol mixture; and  $\triangle$  methanol drops. The straight line is from the numerical simulation of Duchemin *et al.*

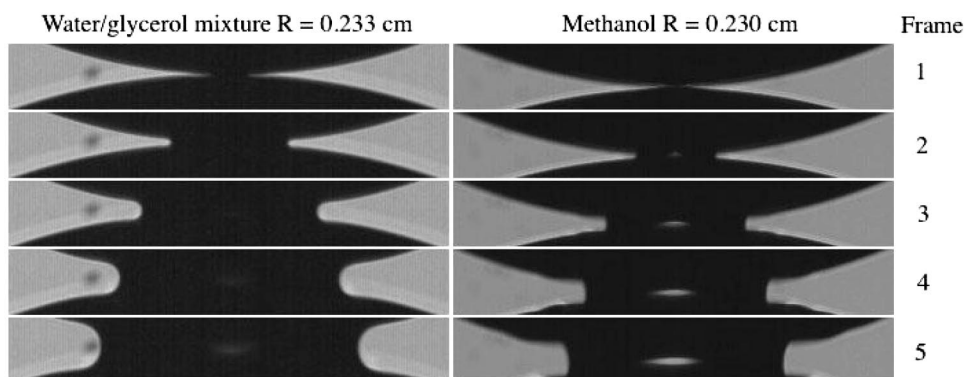


FIG. 6. Time series of images taken by the high speed camera. The time between consecutive frames is  $100 \mu\text{s}$ .

drop. The  $\sim 90^\circ$  corners along the air drop interface near the bridge shown in frames 3, 4, and 5 of methanol drop coalescence (Fig. 6) and of water drop coalescence (Fig. 2) are absent in the case of water–glycerol mixture drop (Fig. 6).

The earlier version of the experiment was carried out on a Teflon coated Plexiglas surface.<sup>12</sup> Liquid (water and water–glycerol mixture) drops are formed on the surface of the substrate by pumping the fluid through two  $120 \mu\text{m}$  diameter holes (2 mm apart) in the Plexiglas substrate via two separate embedded microchannels. The drop size is approximately the same as the distance between the two holes. We found that the early time evolution of the bridge width as well as the air drop interface near the bridge of drop coalescence are similar to those reported above. The scaling law of  $r_b \propto t^{1/2}$  is followed for all the experimental runs. The dimensionless slope is measured to be 1.14–1.33, in which the two drops are not made entirely equal in size. The radius variation ranges from 8–45%.

In summary, we studied experimentally the early time evolution of the liquid bridge formed when two drops merge with negligible velocities in air using water, water–glycerol, mixture, and methanol. The bridge width is found to follow the  $r_b/R \propto (t/\tau)^{1/2}$  scaling law, which agrees well with the theoretical prediction of Eggers *et al.* Using drops of various sizes, we confirmed  $r_b/t \propto R^{1/4}$ . By using three different fluids, we showed that the fluid properties have little influence on the dimensionless scaling law prefactor, however, it does modify the shape of the interface between the air and the drops near the liquid bridge. The experimentally measured dimensionless prefactors (1.29, 1.09, and 1.03) are lower than 1.62, predicted by Duchemin *et al.* for inviscid drop coalescence. It is not clear to us why the dimensionless prefactor for methanol is 20% higher than those of water and water–glycerol mixture. At first, we suspected that it is due to the evaporation of methanol during the experiment. We therefore measured the surface tension of methanol in an

open and a closed environment using a drop volume method. The results excluded such possibility.

Currently, we are studying fluid motion initiated by the rapid release of interfacial stress during the early stage of drop coalescence on a hydrophobic surface of a microfluidic device. The possibilities of using this fluid motion to enhance drop–drop mixing in a microfluidic device is promising, as the Reynolds number of the surface tension driven flow  $\sigma r_b / \rho \nu^2$  can easily reach an order of a few thousands in drop coalescence using low viscosity fluids such as water.

M.W. would like to thank Dr. Jen Eggers for insightful discussions on the subject. This work is supported by the National Science Foundation (CTS-0121340), the Research Corporation (CC4612), and DARPA MPG program.

<sup>1</sup>J. Eggers, “Coalescence of spheres by surface diffusion,” *Phys. Rev. Lett.* **80**, 2634 (1998).

<sup>2</sup>J. Eggers, J. R. Lister, and H. A. Stone, “Coalescence of liquid drops,” *J. Fluid Mech.* **401**, 293 (1999).

<sup>3</sup>L. Duchemin, J. Eggers, and C. Josserand, “Inviscid coalescence of drops,” *J. Fluid Mech.* **487**, 167 (2003).

<sup>4</sup>A. Menchaca-Rocha, A. Martinez-Davalos, R. Nunez, S. Popinet, and S. Zaleski, “Coalescence of liquid drops by surface tensions,” *Phys. Rev. E* **63**, 046309 (2001).

<sup>5</sup>S. T. Thoroddsen, K. Takehara, and T. G. Etoh, “Coalescence of the pendant drops,” *Bull. Am. Phys. Soc.* **48**, 27 (2003).

<sup>6</sup>S. K. Cho, H. Moon, and C.-J. Kim, “Creating, transporting, cutting, and merging liquid droplets by electrowetting-based actuation for digital microfluidic circuits,” *J. Microelectromech. Syst.* **20**, 70 (2003).

<sup>7</sup>P. Paik, V. K. Pamula, and R. B. Fair, “Rapid droplet mixers for digital microfluidic systems,” *Lab Chip* **3**, 253 (2003).

<sup>8</sup>N. Garnier, R. O. Grigoriev, and M. F. Schatz, “Optical manipulation of microscale fluid flow,” *Phys. Rev. Lett.* **91**, 054501 (2003).

<sup>9</sup>S. G. Bradley and C. D. Stow, “Collisions between liquid drops,” *Philos. Trans. R. Soc. London, Ser. A* **287**, 635 (1978).

<sup>10</sup>C. S. Miner and N. N. Dalton, *Glycerol* (Reinhold, New York, 1953).

<sup>11</sup>R. C. Weast, *CRC Handbook of Chemistry and Physics*, 64th ed. (CRC, West Palm Beach, FL, 1985).

<sup>12</sup>M. Wu, T. Cubaud, C.-M. Ho, P.-Y. Chu, and M. C. Wu, “Coalescence of droplets in microfluidic device,” *Bull. Am. Phys. Soc.* **48**, 224 (2003).